Effects of Relatively Insoluble Compounds and β Phase on Stress Corrosion Cracking in 5083 Aluminum Alloy †

Toshio ENJO*, Toshio KURODA** and Hideyuki SHINONAGA***

Abstract

An investigation has been made into the effects of relatively insoluble compounds and β phase on stress corrosion cracking (SCC) in 3.5% NaCl+ 0.5% H_2O_2 solution for Al-Mg series 5083 aluminum alloy. The 5083-O material used for this investigation has rolling texture structure and highly directional grain boundaries.

Therefore, there were much more susceptible to SCC when stress direction was in the short transverse direction (ST) than in the longitudinal direction (L), and consequently it is considered that the lower critical stress on the ST direction specimen is hardly present. The relatively insoluble compounds themselves hardly affect the susceptibility to SCC. On the specimen, the susceptibility to SCC increases as the quantity of β phase increases and the β phase precipitation is accelerated with decreasing in the quantity of relatively insoluble compounds. The susceptibility to SCC on the specimen increases with decreasing in the quantity of relatively insoluble compounds.

In the case of welding by large heat input, SCC occured at the bond area of welds according to above reason. For the SCC, the fracture morphology showed the intergranular fracture with facet pits when β phase hardly precipitates at the grain boundary. The formation of facet pits at the grain boundary decreases with increasing of β phase precipitation at the grain boundary, and the fracture morphology of SCC showed flat intergranualr fracture without facet pits when β phase precipitates at the grain boundary continuously. It is considered that facet pits result from microplasticity at the grain boundary while SCC propagates.

KEY WORDS: (Al Mg Alloys) (Stress Corrosion) (Heat Affected Zone) (Metallography),(Fractography)

1. Introduction

Al-Mg series 5083 aluminum alloy has characterized by ease of welding and good resistance to stress corrosion cracking.

Therefore, it has been widely used for various weldments such as viecle and LNG tank. Recently, plates of thickness above 50 mm have been used for large weldments that involved butt and fillet welds. Then we have to consider not only mechanical properties and stress corrosion cracking resistance of longitudinal direction (L) up to now but also those of short transverse direction (ST).

Because the alloy has rolling texture structure and highly directional grain boundaries.

β phase (Mg_2Al_3) precipitates at the grain boundary during aging process[1) 2)] and this phase is considered as one of causes for stress corrosion cracking. β phase is anodic on electric potential as compared with matrix, therefore it is said that the dissolution area of β phase is paths of stress corrosion cracking[3) 4)] The other side, additive elements such as Mn,Cr and so on are known to have an effect on improving to stress corrosion cracking.[5)] That is, relatively insoluble compounds precipitated owing to their additive elements during process of homogenized treatment are considered to be effective for stress corrosion cracking.

In the case of welding of the alloy, their relatively insoluble compounds precipitate or solutionize at the area heated up to the melting point such as weld bond area, and their compounds influence upon following precipitation behavior of β phase during cooling.[6) 7)]

Then, the present investigation has been made into the effects of relatively insoluble compounds and β phase on stress corrosion cracking by the metallographic observation of the fracture surface due to stress corrosion cracking.

2. Experimental procedures

Chemical compositions of 5083-O material used are

† Received on March 31, 1979
* Professor
** Research Instructor
*** Graduate Student, formerly (Tokyo Shibaura Electric Co., Ltd.)

Table 1 Chemical compositions (wt%) and plate thickness (mm) of material used.

	Cu	Si	Fe	Mn	Mg	Zn	Cr	Ti	Zr	Al	
5083	0.02	0.15	0.20	0.64	4.7	0.01	0.11	0.01	—	Bal.	6 2[t]

shown in **table 1**. For heat treatment of material used, silicone oil bath below 200°C and salt bath in the range 200°C to 560°C were used respectively.[6) 7)] Design and positions of extraction for specimens with V notch used in the stress corrosion cracking are shown in **Fig. 1**. Stress

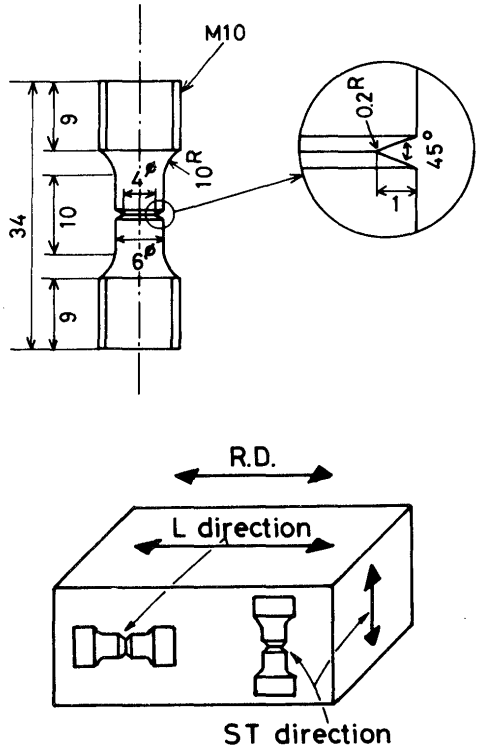

Fig. 1 Design, and positions of extraction for specimen with V notch used in SCC test

corrosion cracking test was carried out in 3.5% NaCl + 0.5% H_2O_2 solution using dead weight type machine, and the applied load and fracture time were recorded using pen recorder.

PH of the solution was about 4.5 for the first time of stress corrosion cracking test. The specimen was washed by ultrasonic vibration in acetone solution, and was coated with vinyl tape and paint except notched portion. The fracture surface obtained was observed in detail using scanning electron microscope.

Microscopic structure was obtained by etching in 20% phospholic acid solution.

3. Results and Discussions

3.1 Relationship between rolling texture structure and stress corrosion cracking.

Fig. 2 shows the stress corrosion cracking curves in 3.5% NaCl + 0.5% H_2O_2 solution for L direction, ST direction and 45 degree specimen respectively. Notch

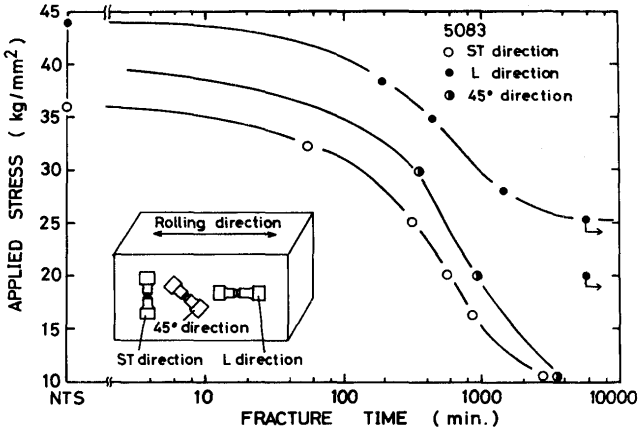

Fig. 2 Stress corrosion cracking curves in 3.5% NaCl + 0.5% H_2O_2 solution for specimens extracted from plate with various directions.

tensile strength (NTS) of L direction specimen was 44 kg/mm^2, otherwise that of ST direction specimen was 36 kg/mm^2, namely, NTS of ST direction specimen was 8 kg/mm^2 lower than that of L direction specimen. On the stress corrosion cracking, lower critical stress at which stress corrosion cracking is not occured even for 100 hours, is about 25 kg/mm^2 for L direction specimen but stress corrosion cracking of ST direction and 45 degree direction specimen occured even at applied stress of 10 kg/mm^2, therefore lower critical stresses for their specimens are considered not to be present. The fracture time of stress corrosion cracking becomes shorter as the direction of stress becomes to rectangular to rolling texture structure such as ST direction and 45 degree specimen. The specimen has V notch, and then the notch root area is over the yield stress even at nominal applied stress of 10 kg/mm^2. Because the yield stress of L direction and ST direction specimens was both about 15 kg/mm^2.

Then we made the plain specimen, and carried out stress corrosion cracking test at applied stress (about 7 kg/mm^2) of 50% of yield stress for 2 days. And, after removal of applied stress, microstructures showing stress corrosion cracking profile were observed for various specimens' sections. Their results are shown in **Photo. 1**. We could hardly recognize effect of stress corrosion for L direction specimens. But we could recognize that stress corrosion occured along the grain boundaries even at

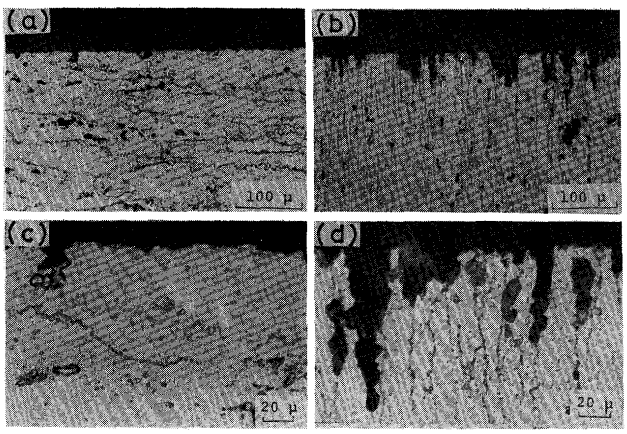

Photo. 1 Microstructures showing corrosion profile in 3.5% NaCl + 0.5% H_2O_2 solution for L direction specimen (a), (c) and ST direction specimen (b), (d) for 5083-O material used.

applied stress of 7 kg/mm^2, consequently the lower critical stress of stress corrosion cracking is considered not to be present for ST direction specimen.

3.2 Relationship between solution temperature and stress corrosion cracking

When the material used in the present investigation is welded, the welds is heated above solution temperature of β phase, and precipitation or solution of relatively insoluble compounds occurs.[6) 7)] Then in this section, a study has been made into the effect of solution treatment temperature on the stress corrosion cracking. **Fig. 3** shows

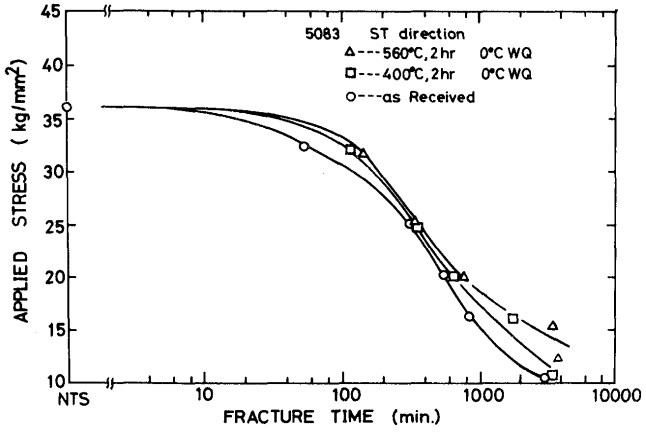

Fig. 3 Stress corrosion cracking curves in 3.5% NaCl + 0.5% H_2O_2 solution for ST direction specimens heat-treated at various solution temperatures.

the results of stress corrosion cracking for ST direction specimens heat-treated at various solution temperatures. The β phase has precipitated a few from the matrix in as-received material due to annealing. Therefore, the fracture time of as-received material is a few shorter than that of solution treatment. This alloy contains additive elements such as Cr,Mn so on in order to inhibit recrystallization and to improve stress corrosion cracking, and relatively insoluble compounds of $Al_{18}Cr_2Mg_3$, Al (Fe,Mn) Si so on precipitated during homogenized heat treatment are present.[7)] Their compounds have precipitated more at 400°C solution temperature but solutionized above 500°C solution temperature.[7)] Consequently, precipitation amount of relatively insoluble compounds changed with solution temperature. But as shown in Fig. 3, stress corrosion cracking curves are hardly changed with the amount of relatively insoluble compounds. Therefore, it appears to as that the relatively insoluble compounds themselves hardly affect the susceptibility to stress corrosion cracking.

3.3 Effect of β phase precipitation on stress corrosion cracking

It is known that β phase precipitation at the grain boundary affects stress corrosion cracking on Al-Mg series 5083 alloy.[1) 2) 3) 4)].

Then, **Fig. 4** and **Fig. 5** show the change in the fracture

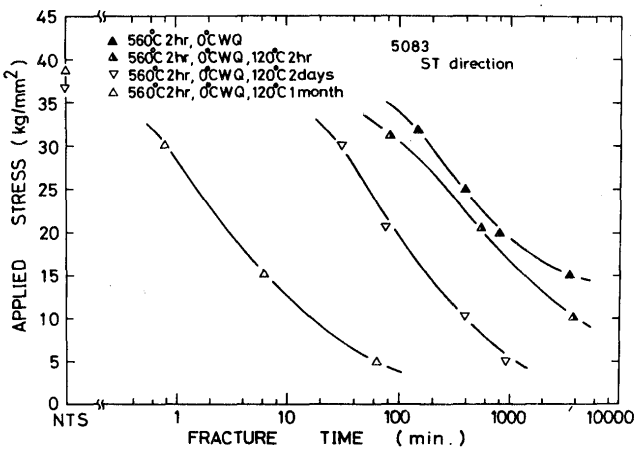

Fig. 4 Stress corrosion cracking curves in 3.5% NaCl+ 0.5% H_2O_2 solution for ST direction specimens aged at 120°C after solution heat treatment at 560°C

time by stress corrosion cracking when specimens were aged at 120°C after water quench from heat treatment temperature of 400°C and 560°C respectively. On both specimens heat-treated at 400°C and 560°C, the fracture times by stress corrosion cracking reduce with increasing of aging time at 120°C. **Fig. 6** shows the stress corrosion cracking curves for ST direction specimens aged at 120°C for 1 month after solution heat treatment at various

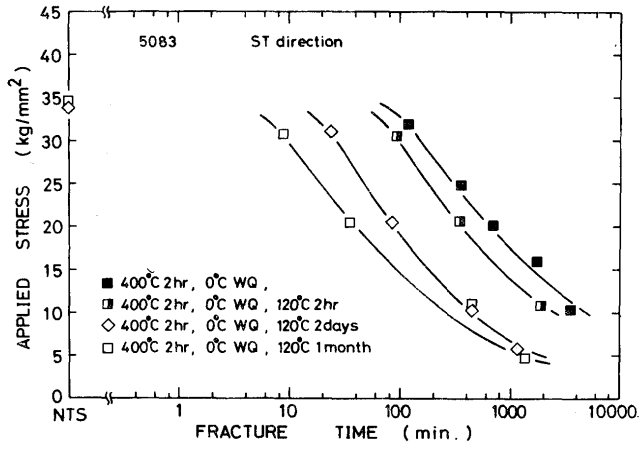

Fig. 5 Stress corrosion cracking curves in 3.5% NaCl + 0.5% H_2O_2 solution for ST direction specimens aged at 120°C after solution heat treatment at 400°C.

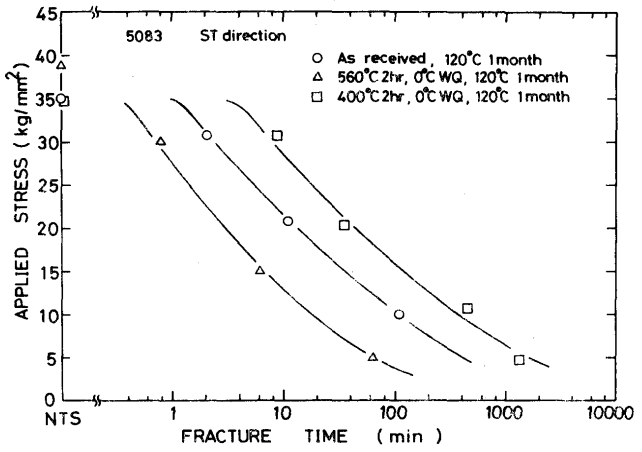

Fig. 6 Stress corrosion cracking curves in 3.5% NaCl + 0.5% H_2O_2 solution for ST direction specimens aged at 120°C for 1 month after solution heat treatment at various temperatures.

temperatures. When the solution temperature is high and relatively insoluble compounds are solutionized, β phase precipitation at the grain boundary by 120°C aging becomes more[7], therefore the fracture time becomes shorter. Precipitation of relatively insoluble compounds contained in 5083-O material is less than that of 400°C heat-treated specimen and solution of the compounds in 5083-O material is less than that of 560°C heat-treated specimen. Consequently, the fracture time of 5083-O material is just intermediate between those of the heat treatment specimens. According to the report of Dix etc.[10], β phase precipitates at the grain boundary during aging process at 100°C ~ 150°C and so even by natural aging for 24 years. And this report is discussed for the case of usual 450°C solution treatment

As it is expected that the precipitation of β phase is accelerated at the weld bond area, we have to take notice of this point enough at the planning stage for marine application.

β phase precipitation at the grain boundary is dangerous for stress corrosion cracking, but the NTS at room temperature is hardly affected by β phase precipitation as shown in Fig 4 and Fig 5.

Considering to use it at low temperature so as LNG tank, we studied the effect of β phase precipitation on NTS at −196°C.

The results showed that NTS of material aged at 120°C for 1 month is same as that of as-received material for L direction specimen and ST direction specimen. Consequently, it was evaluated that the precipitation of β phase at the grain boundary hardly affected the NTS at various temperatures.

3.4 Relationship between weld heat input and stress corrosion cracking.

Recently, as the weldments became larger, the plate of thickness above 50 mm has been widely used. And the welding has been carried out using GMA (MIG) or GTA (TIG) of large current in order to increase efficiency. Then an investigation has been made into the stress corrosion cracking of welds based on above results and experiment results are discussed in this section. The welding was made by bead-on-plate method of TIG welding. For the welding condition, welding voltage was 23 V, welding current was 430 A, welding speed was 20 cm/min. and weld heat input was 30000 J/cm. We extracted the plain specimen (6 mm ϕ, gauge length 50 mm) from the welded plates.

The deposit metal zone was placed at the middle area of gauge length. Well, welding direction is parallel to rolling direction of plate. **Fig. 7** shows the stress

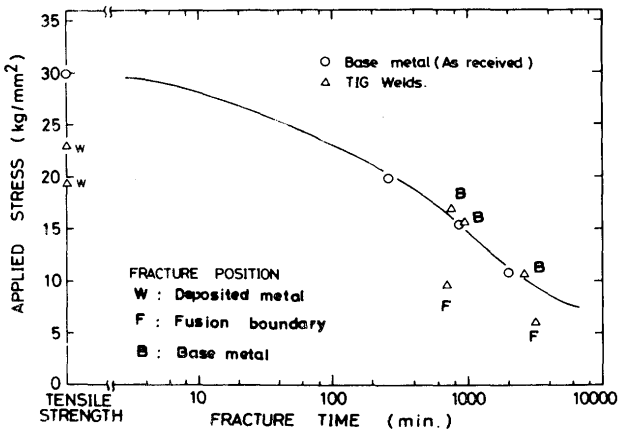

Fig. 7 Stress corrosion cracking curves in 3.5% NaCl + 0.5% H_2O_2 solution for LT direction specimens of base metal and TIG welds.

corrosion cracking curves for LT direction specimens of base metal and TIG welds. When applied stress is high, the fracture time of welds was same as that of base metal, and the fracture position was area heated near the solution temperature. When applied stress is low, the fracture time of welds was shorter than that of base metal and the fracture position was bond area (fusion line). Namely, for welding of large heat input, the near by bond is heated to high temperature, and the relatively insoluble compounds is considerably solutionized, following β phase precipitation is accelerated during slow cooling.[7] Consequently, it is considered that stress corrosion cracking of welds occured at the bond area. Then, stress corrosion cracking test of electron beam welds was carried out. For condition of electron beam welding (EBW), welding voltage, welding current, welding speed, were 10 kV, 40 mA, 60 cm/min. respectively. Stress corrosion cracking curve of the welds was same as that of base metal, and the fracture position of welds was at the base metal. Because EBW is low heat input of 1000 J/cm and the thermal cycle is too fast, β phase hardly precipitates during the cooling.

Photo. 2 shows the fracture appearance of stress

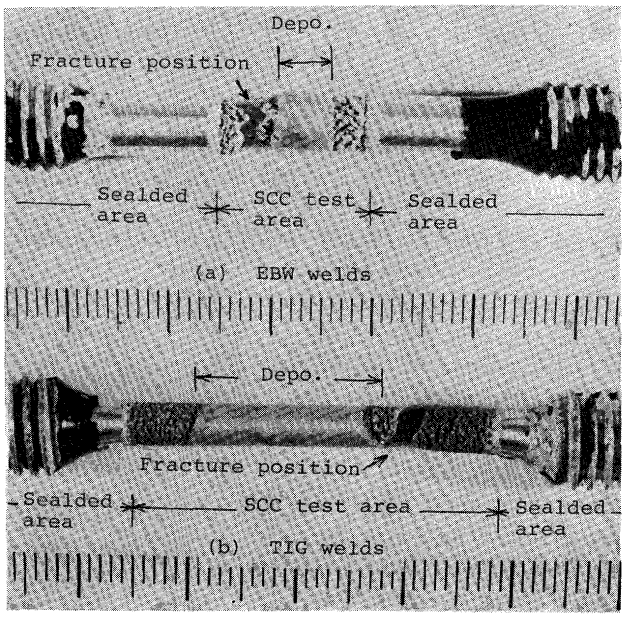

Photo. 2 Fracture appearance of SCC in EBW welds and TIG welds.

corrosion cracking in EBW welds and TIG welds. On EBW welds, the fracture occured at the base metal but on TIG welds crack initiated at the bond area and propagated into the base metal. At the left hand of deposit metal, the crack initiated and propagated along the bond area. Niederberger etc[5]. pointed out that bond area (fusion line) of the welds was corroded preferentially but the base metal was hardly corroded on commercially Al-Mg alloy welds in the case of immersion into sea water. This report proves the present results which show that β phase has precipitated preferentially at the bond area of welds and the fracture occured in the place.

3.5 Pit formation on fracture morphology of stress corrosion cracking.

It is known that stress corrosion cracking of aluminum alloys shows intergranualr fracture type. Then, an investigation has been made into the relationship between β phase precipitation at the grain boundary and fracture morphology of stress corrosion cracking. And the results of examination are discussed in this section. **Photo. 3** shows the microstructure showing crack profile of stress corrosion cracking in 3.5% NaCl + 0.5%H_2O_2 solution for

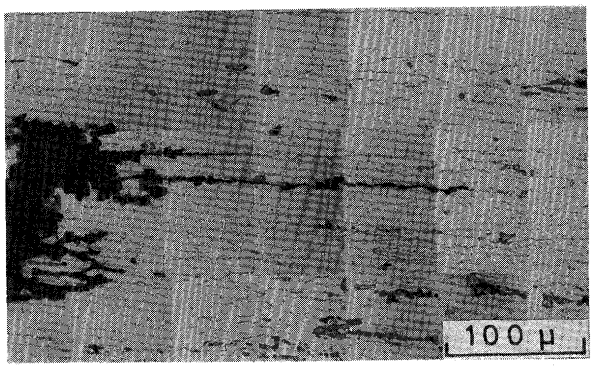

Photo. 3 Microstructure showing crack profile of SCC in 3.5% NaCl + 0.5% H_2O_2 solution for ST direction specimen of 5083-O material used.

ST direction specimen of 5083-O material. Left side of the photograph is crack initiation site. The corrosions have occured considerably in plastic deformation area of notch root and cracks along the grain boundary have propagated preferentially into the inside of specimen. Pits of square type are formed around the crack. This crack is considered to lead to rupture of stress corrosion cracking. **Photo. 4** shows the fracture morphology of stress corrosion cracking for ST direction specimens of 5083-O material used. Mark A is notch root area, Mark B is stress corrosion cracking area and Mark C is rapid fracture area as shown in Photo. 4-(a). We can distinguish to stress corrosion cracking area from rapid fracture area. As shown in Photo. 4-(b), the fracture morphology of stress corrosion cracking area (A) showing intergranular fracture is different from that of rapid fracture area (B) showing dimple fracture which initiates at relatively insoluble

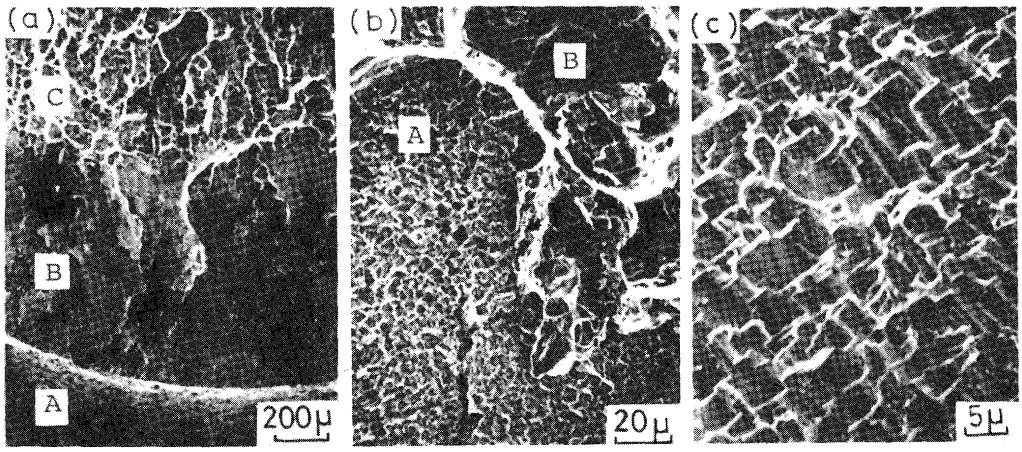

Photo. 4 Fractographs of SCC for ST direction specimens of 5083-O material used.

compounds and inclusions. Fracture morphology of stress corrosion cracking is occupied with pit formation as shown in Photo. 4-(c) enlarged stress corrosion cracking area. **Photo. 5** shows the fracture morphologies of stress corrosion cracking for L direction specimens of 5083-O material. As shown in Photo. 5-(a), the stratified fracture morphology is observed in stress corrosion cracking area because many subcracks propagated parallel to stress direction and these subcracks propagated along the flat grain boundary which occured by rolling process. Photo. 5-(b) shows the photograph enlarged Photo. 5-(a). The pit shapes are same as that of Photo. 4-(c) of ST direction specimen. Consequently, these pits are considered to be facet pits which have crystallographic orientation. Then, in order to evaluate the formation process of facet pits, following experiments were carried out. In order to obtain the intergranular fracture surface in 5083-O material, as shown in **Photo. 6-(a),** Charpy impact test specimens were cut off from the plate and impact test was carried out at $-196°C$. As the results, as shown in Photo. 6-(a), we could obtain fracture morphology of intergranular type which occured stepwise along the grain boundary. This fracture surface was immersed in 3.5% NaCl + 0.5% H_2O_2 solution for 24 hours, and then the fracture surface was observed using scanning electron microscope. The results are shown in **Photo. 6-(b)** and **(c).** The fracture morphology shows still flat intergranular fracture and the facet pits hardly formed on the grain boundary. Therefore, it is considered that facet pits shown in Photo. 4 was not occured by prolonged immersing in the solution after fracture of stress corrosion cracking but occured during propagation process of stress corrosion cracking. **Photo. 7** shows the change in fracture morphology of ST direction specimen with increasing of aging time. These specimens were solutionized at 560°C for 2 hours, and

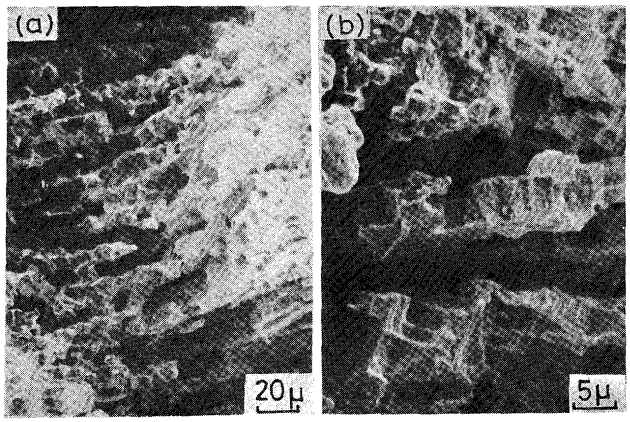

Photo. 5 Fractographs of SCC for L direction specimens of 5083-O material used.

aged at 120°C for 2 hours, 2 days and 1 month respectively. For 2 hours aging, as shown in Photo. 7-(a), the facet pits are present on all grain boundaries. For 2 days aging, as shown in Photo. 7-(b), the facet pits are observed considerably on the fracture surface, but flat intergranular fracture morphology is partially observed. For 1 month aging, as shown in Photo. 7-(c), the facet pits are not observed on the intergranular fracture surface. It is well known that β phase precipitates discontinuously at the grain boundary for the first aging time at 120°C, and precipitates continuously at the grain boundary as aging time increases. Consequently, it is suggested that precipitation area of β phase at the grain boundary shows flat intergranular fracture morphology, and when the precipitation of β phase at the grain boundary is still less, intergranular fracture morphology with facet pits is obtained. **Photo. 8** shows the fracture morphology showing microplasticity on the intergranular fracture

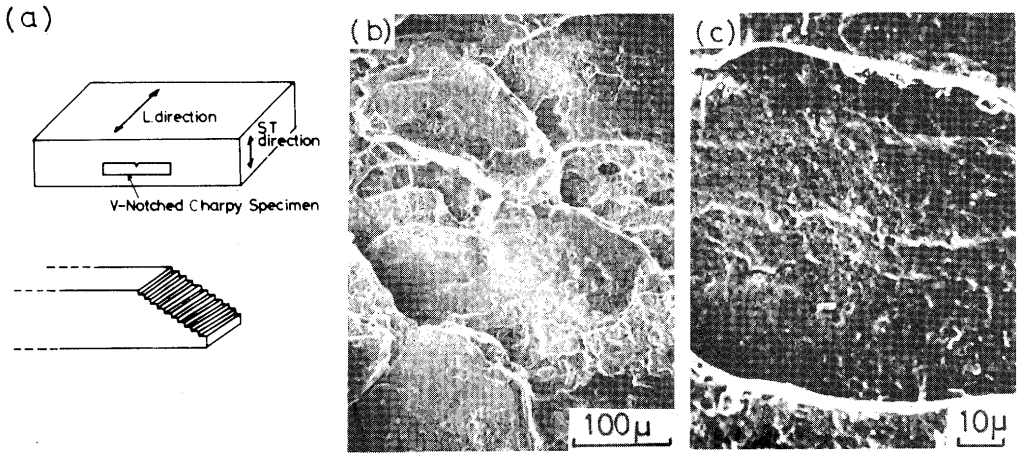

Photo. 6 Fractographs showing intergranular fracture for the specimen fractured at −196°C and then immersed in 3.5% NaCl + 0.5% H_2O_2 solution for 24 hours.

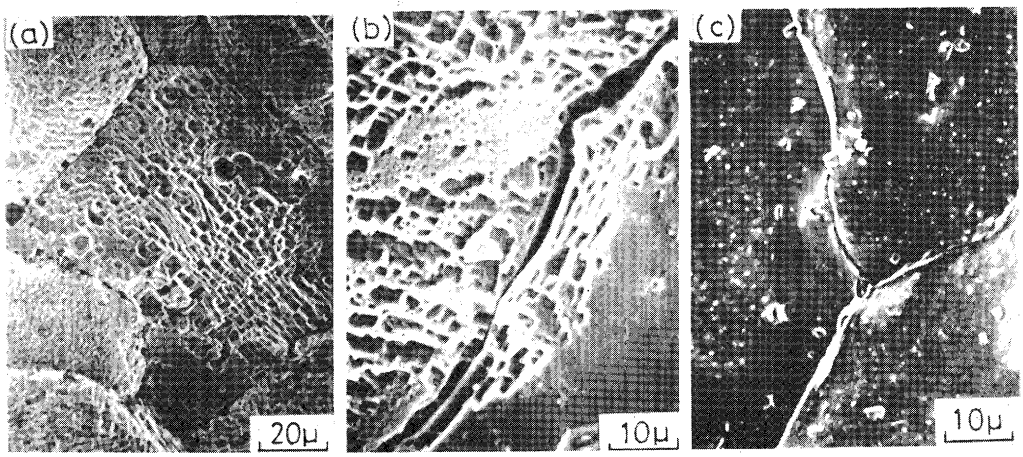

Photo. 7 Effect of aging time at 120°C on the fracture morphology of SCC. (a) 2 hours aging (b) 2 days aging (c) 1 month aging

surface by stress corrosion cracking at high applied stress, for ST direction specimen and L direction specimen heat-treated at 120°C for 1 month after 560°C solution treatment.

Notch area is general yielded at the applied stress of 17 kg/mm^2 by means of elasitc-plastic analysis by finite elements method for the specimen dimension used. Consequently, the fracture morphology shows the flat intergranular fracture without facet pits, and many slide lines observed on the intergranular fracture surface. Generally, orientation pit is related with dislocation, and occurs at the fracture area of oxide film and working crack.

When plastic deformation occued by applied stress,

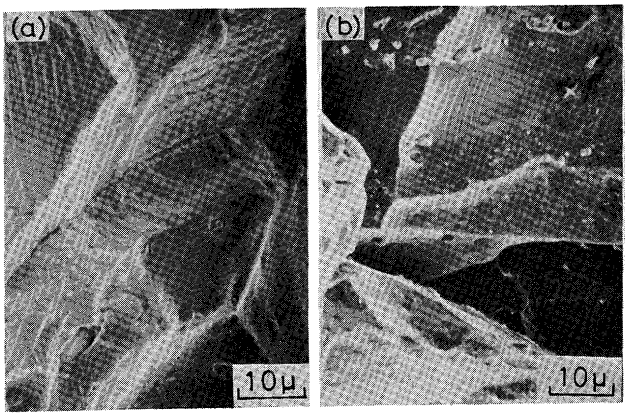

Photo. 8 Fractographs showing microplasticity on the intergranular fracture surface by SCC. (a) L direction (b) ST direction

many pits occur on the slide lines. Therefore, as many slide lines were observed on the intergranular fracture surface, the formation of facet pits were expected. But we couldn't observe facet pits on the fracture surface. This phenomena is considered to occur by following cause. Namely, the facet pits are formed by microplasticity near the grain boundary during crack propagation in the corrosion environment, and prior plastic deformation by applied stress doesn't affect the formation of facet pits.

Generally, mechano-chemical theory and dissolution theory are roughly proposed as mechanism of stress corrosion cracking. If intergranular fracture shown in Photo. 7 (c) occured by dissolution of β phase at the grain boundary, the fracture morphology is expeced to be different from general intergranular fracture morphology.

Then **Photo. 9** shows the fracture morphology of ST direction specimen fractured at $-196°C$. The specimen is solution heat treated at 560°C for 2 hours and then aged at 120°C for 1 month.

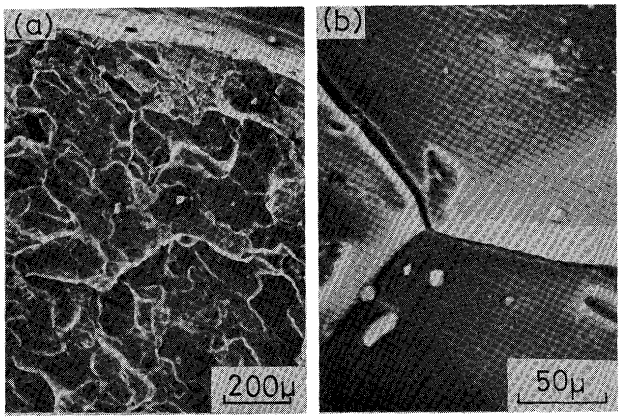

Photo. 9 Fractographs showing intergranular fracture of ST direction specimen fractured at $-196°C$, after solution heat treatment at 560°C for 2 hours and then aging treatment at 120°C for 1 month.

The fracture morphology shows flat intergranular fracture as shown in Photo. 9-(a). Photo. 9-(b) enlarged photograph of Photo. 9-(a) shows the flat intergranular fracture as same as Phto. 7-(c).

Consequently, the statement that β phase precipitates at the grain boundary continuously, couldn't be evaluated from fractography.

NTS at $-196°C$ was 46 kg/mm^2 but stress corrosion cracking occured even at applied stress of 5 kg/mm^2. Therefore it is difficult to explain this phenomena by only grain boundary embrittlement owing to β phase precipitation. Preferably, the phenomena is considered that β phase dissolution at the grain boundary occured during crack propagation of stress corrosion cracking. Namely, it is considered that cracks propagated by preferential dissolution of β phase, the stress necessary to fracture along the grain boundary is low, the crack propagated without plastic deformation, and then pit formation didn't occur. **Photo. 10** shows the fracture

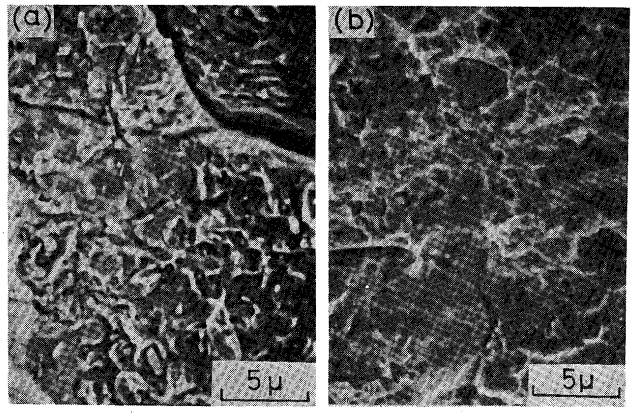

Photo. 10 Fractographs of SCC (a) and tensile fracture at $-196°C$ (b) for the specimen aged at 120°C for 1 month after solution heat treatment at 400°C for 2 hours.

morphologies of stress corrosion cracking (a) and tensile fracture at $-196°C$ (b) for ST direction specimen aged at 120°C for 1 month after solution heat treatment at 400°C for 2 hours. Both fracture surfaces show the intergranular fracture morphology. The recrystallization doesn't occur and the more relatively insoluble compounds precipitate for this solution treatment. Therefore, the fracture morphology shown in Photo. 10-(a) is different from flat intergranular fracture morphology shown in Photo. 7-(c) and Photo. 6. This phenomena suggests that precipitation behavior of β phase is affected by the precipitation of relatively insoluble compounds.

4. Summary

An investigation has been made into the effects of relatively insoluble compounds and β phase on stress corrosion cracking in 5083 aluminum alloy. The results obtained in this investigation are summerized as follows.

(1) 5083-O material used in this investigation has rolling texture structure and highly directional grain boundaries. The lower critical stress of longitudinal direction specimen is high for SCC and the specimen has a good resistance to SCC , but that of short transvers direction specimen is hardly present. Consequently, for use of this alloy as structural material, this material has to be considered enough

for stress direction at the planning base.

(2) The relatively insoluble compounds themselves hardly affect the susceptibility to SCC. The susceptibility to SCC increases with increasing of β phase precipitation.

(3) β phase precipitation is accelerated with decreasing in the quantity of relatively insoluble compounds. In the case of welding by large heat input, the relatively insoluble compounds are solutionized considerably and β phase precipitates more at weld bond area. Consequently, SCC of the welds occured at the bond area.

(4) When β phase hardly precipitates at the grain boundary, the fracture morphology of SCC showed the intergranualr fracture with facet pits. The formation of facet pits at the grain boundary decreases with increasing of β phase precipitation at the grain boundary. When β phase precipitated at the grain boundary continuously, the fracture morphology of SCC showed flat intergranular fracture without facet pits. Consequently, it is considered that facet pits results from microplasticity at the grain boundary while SCC propagates.

Acknowlegements

The authours wish to thank Mr. M. Nakamura and Mr. T. Horinouchi for their variable contributions in this work. The support of the Light Metal Educational Foundation is grately acknowledgement.

References

1) E.C.W. Perryman and G.B. Book: Mechanism of Precipitation in aluminum-magnesium alloys, J. Inst. of Metals, 79, (1951) 19
2) A. Eikum and G. Thomas: Precipitation and dislocation nucleation in quenched-aged Al-Mg alloys, Acta Met. 12 (1964) 537
3) W.W. Binger, E.H. Hollingsworth and D.O. Sprowls: Aluminum, (Kent R. Van Horn, ed) 1, ASM (1967) 209
4) E.C.W. Perryman and S.E. Hadden: Stress corrosion of Al-7%Mg alloy, J. Inst. of Metals, 77 (1950) 207
5) R.B. Niederberger, J.L. Basil and G.T. Bedford: Corrosion and stress corrosion of 5000 series aluminum alloys in marine environments, Corrosion, 22 (1966) 68
6) T. Enjyo, T. Kuroda and H. Shinonaga: J. of Light Metal Welding and Construction, 69, (1978) 393 (in Japanese)
7) T. Enjyo, T, Kuroda and H. Shinonaga: Effect of relatively insoluble compounds on β phase precipitation in 5083 aluminum alloy, Trans of JWRI, 7 (1978) 173
8) T. Ohnishi and Y. Nakatani: Effects of some factors on stress corrosion susceptibility of Al-Mg alloys, J. of Japan Inst. of Light Metals, 26 (1976) 18 (in Japanese)
9) E.G. Coleman, D. Weinstein and W.R. Rostokev: On a surface energy mechanism for stress-corrosion cracking, Acta Met. 9 (1961) 491
10) E.H.Dix, JR, W.A. Anderson and M.B. Shumaker: Influence of service temperature on the resistance of wrought aluminum-magnesium alloys to corrosion, Corrosion, 15, (1959) 55t
11) J.J. Harwood: Stress corrosion cracking and embrittlement John Wiley and Sons, New York (1959) 1
12) T. Ohnishi, Y. Nakatani and H. Sakamoto: Effect of microstructure on stress corrosion susceptibility of Al-Mg alloy, J. Japan Inst. of Light Metals, 26, (1976) 8 (in Japanese)
13) H.H. Uhlig: Physical metallurgy of S.C.F., Interscience Publishers, New York (1959). 1